ESTIMATION OF PHASE CONSTRAINED MIMO TRANSFER FUNCTIONS WITH APPLICATION TO FLEXIBLE STRUCTURES WITH MIXED COLLOCATED AND NON-COLLOCATED ACTUATORS AND SENSORS

Tomas McKelvey * and **S. O. Reza Moheimani** **

* *Dept. of Signals and Systems, Chalmers University of Technology, SE-412 96 Gothenburg, Sweden, mckelvey@s2.chalmers.se*
** *Dept. of Electrical and Computer Engineering, University of Newcastle, Newcastle, Australia.*

Abstract: A computational scheme is proposed to estimate a state-space representation of MIMO transfer functions from frequency response measurements. The approach can constrain the phase curve of selected elements of the transfer function matrix to certain regions. Poles of the system are determined using a frequency domain subspace approach. The phase constraint is enforced by an LMI formulation based on the positive real lemma when the zeros of the system are estimated. The successful application of the algorithm to measurements from a cantilever beam with three collocated piezoelectric actuator/sensor pairs is demonstrated.

Keywords: Subspace method, system identification, flexible structures, positive real transfer functions, LMI

1. INTRODUCTION

Experimental modeling of dynamical systems is often used to obtain simple and accurate models of complex structures. Finite dimensional models play a particularly important role for many successful applications of model-based signal processing and model-based control design. In this paper we will present a system identification method which estimates linear dynamical MIMO systems from either frequency response function (FRF) data or samples of the Fourier transform of the input and output signals.

The main contribution of the paper is to demonstrate how phase constraints of certain transfer function elements, dictated by the physical system which is modeled, can be enforced directly in the identification procedure. Flexible structures with collocated sensors and actuators have the particular property that the (ideal) transfer function between the actuator and sensor is positive-real. A square transfer function $\Psi(\omega)$ is *positive-real* if for $\omega \in \mathbb{R}$

$$\Psi(\omega) + \Psi(\omega)^* \geq 0 \tag{1}$$

However, depending on the nature of the signals measured by the sensors, or actuation mechanism, the actual transfer function may include a derivative or an integral of the "physical" transfer function. This will add or subtract 90 degrees of the phase curve, which renders the positive real transfer function (for $\omega \geq 0$) *positive imaginary* or *negative imaginary* respectively.

In this paper we will identify state-space models of the form

$$\begin{aligned} \dot{x} &= Ax + Bu \\ y &= Cx + Du \end{aligned} \tag{2}$$

where $u \in \mathbb{R}^m$ is vector of inputs while $y \in \mathbb{R}^p$ is the vector of outputs and $x \in \mathbb{R}^n$ is the state-vector. Furthermore, we will assume that certain elements of the frequency function matrix

$$G(\omega) = D + C(j\omega I - A)^{-1}B \tag{3}$$

have phase curves which are constrained to certain regions of the complex plane. That is, we assume a set of $p = 1, \ldots, n_c$ index pairs i_p, j_p where each of the n_c transfer function elements

$$G_{i_p,j_p}(\omega) = D_{i_p,j_p} + C_{i_p}(j\omega I - A)^{-1}B_{j_p} \tag{4}$$

satisfy the phase constraint

$$\angle G_{i_p,j_p}(\omega) \in \mathscr{P}_p, \quad \forall \omega > 0. \tag{5}$$

where $\mathscr{P}_p$ is one of the four sets

$$\begin{array}{ll} \mathscr{P}^{\mathrm{PR}} = [-\frac{\pi}{2}, \frac{\pi}{2}], & \mathscr{P}^{\mathrm{NR}} = [\frac{\pi}{2}, \frac{3\pi}{2}], \\ \mathscr{P}^{\mathrm{PI}} = [0, \pi], & \mathscr{P}^{\mathrm{NI}} = [\pi, 2\pi] \end{array} \tag{6}$$

where the superscripts P and N stand for positive and negative and R and I denote real and imaginary respectively. Note that within the formulation above, constraints representing the phase of the four quadrants of the complex plane, can be constructed by combining two half-plane constraints for the same transfer function element. For example the constraint $[0, \pi/2]$ is obtained by combining $\mathscr{P}^{\mathrm{PR}}$ and $\mathscr{P}^{\mathrm{PI}}$. Hence, a total of 8 meaningful phase constraints can be represented.

The proposed scheme for estimating this class of models consists of the following two main steps:

(i) An estimate of the A and C matrices of the state-space model (2) is calculated using a subspace based approach.
(ii) Estimates of the B and D matrices are found by minimizing a least-squares criterion subject to the set of phase constraints dictated by the system structure.

The division in two separate steps facilitates the task of estimation and makes it possible to calculate the estimate without the need for applying Newton-type nonlinear programming with constraints. Furthermore, from a mechanical structural dynamics point of view the division is also natural. The eigenvalues of the A matrix are the poles of the system which dictates the global dynamics in the overall structure and are not dependent on the actual placement of the actuators and sensors. Hence, the location of the eigenvalues is completely decoupled with the issue of phase constraints since the shape of the phase curve is directly related to the zeros of the transfer function elements.

The proposed approach makes use of the well known Positive Real Lemma e.g. (Rantzer, 1996) to formulate the phase constraints. Similar techniques have been used in (Stoica *et al.*, 2000; Mari *et al.*, 2000; Van Overschee *et al.*, 1997) for the estimation of spectral models and in (Jesse *et al.*, 2004) for identification of continuous time positive real models operating under zero-order hold conditions. In (Goethals *et al.*, 2003) a regularization approach for identification of positive real models have been suggested.

The paper is organized as follows. In the next section we show how the phase constraints can be formulated as the feasibility of a linear matrix equality (LMI). In the section that follows we show how the poles of the system are identified using a frequency domain subspace method. In Section 4 we show how to solve the least-squares problem for estimating B and D matrices subject to the phase constraint by coupling the LMI formulation with second order cone programming. An example is then presented where a 3 x 3 linear model of a cantilever beam is estimated from measurement data. The concluding section then summarizes the contributions.

2. PHASE CONSTRAINTS AND THE POSITIVE REAL LEMMA

In this section we will explain how the phase constraints in (6) can be formulated as the feasibility of a set of linear matrix inequalities. A key result in the derivations is the well known Positive Real Lemma.

Lemma 1. (PR). Given $A \in \mathbb{R}^{n\times n}$, $B, C^T \in \mathbb{R}^{n\times m}$, $D \in \mathbb{R}^{m\times m}$, with $\det(j\omega I - A) \neq 0$ for $\omega \in \mathbb{R}$, (A,B) controllable and $\Psi(\omega) = D + C(j\omega I - A)^{-1}B$, the following two statements are equivalent:

i For $\omega \in \mathbb{R}$

$$\Psi^*(\omega) + \Psi(\omega) \geq 0 \tag{7}$$

ii There exists $P = P^T \in \mathbb{R}^{n\times n}$ such that

$$\begin{bmatrix} PA + A^T P & PB + C^T \\ B^T P + C & D + D^T \end{bmatrix} \geq 0 \tag{8}$$

A proof of the result can be found in many publications, e.g. (Rantzer, 1996). A dual of this result can be obtained by finding the Hermitian transpose of the transfer function.

Lemma 2. (PR dual). Given $A \in \mathbb{R}^{n\times n}$, $B, C^T \in \mathbb{R}^{n\times m}$, $D \in \mathbb{R}^{m\times m}$, with $\det(j\omega I - A) \neq 0$ and (A,C) observable and $\Psi(\omega) = D + C(j\omega I - A)^{-1}B$, the following two statements are equivalent:

i For $\omega \in \mathbb{R}$

$$\Psi^*(\omega) + \Psi(\omega) \geq 0 \tag{9}$$

ii There exists a $P = P^T \in \mathbb{R}^{n\times n}$ such that

$$\begin{bmatrix} PA^T + AP & B + PC^T \\ B^T + CP & D + D^T \end{bmatrix} \geq 0 \tag{10}$$

In the remainder of the paper we will restrict the discussion to scalar transfer functions. Hence the inequality (7) equals the $\mathscr{P}^{\mathrm{PR}}$ (positive real) phase constraint. A scalar transfer function is thus guaranteed to be positive real if the LMI (10) (or (8)) is feasible, i.e. there exists a P such that the matrix expression is positive semidefinite. Note that the LMI is an affine function of the P,B and D (or P,C and D) matrices. This observation is important when we wish to couple the LMI feasibility problem with the least-squares estimation of the B and D (or C and D) matrices. We will return to the computational issues later on. To this end, we point out that if $\Psi(\omega)$ is positive real then obviously $-\Psi(\omega)$ is negative real. Consequently, for the $\mathscr{P}^{\mathrm{NR}}$ (negative real) phase constraint, the LMI (10) can be used by substituting $D \to -D$ and $B \to -B$ (or $D \to -D$ and $C \to -C$ for (8)).

Formulating LMI feasibility tests for the $\mathscr{P}^{\mathrm{PI}}$ and $\mathscr{P}^{\mathrm{NI}}$ constraints requires a few manipulations. We have the following new result.

Lemma 3. (PI-NI Lemma). Given $A \in \mathbb{R}^{n\times n}$, $B, C^T \in \mathbb{R}^n$, $D \in \mathbb{R}$, with $\det(j\omega I - A) \neq 0$ and (A,C) observable, $\Psi(\omega) = D + C(j\omega I - A)^{-1}B$ and $\Phi_R(\omega) = CA^{-1}(j\omega I - A)^{-1}B$. Then for $\forall \omega > 0$

i $\mathrm{Im}[\Psi(\omega)] \geq 0$ if and only if $\mathrm{Re}[\Phi_R(\omega)] \geq 0$.
ii $\mathrm{Im}[\Psi(\omega)] \leq 0$ if and only if $\mathrm{Re}[\Phi_R(\omega)] \leq 0$.

Proof: First notice that for $\omega > 0$, $\mathrm{Im}[\Psi(\omega)] \geq (\leq) 0 \Leftrightarrow \mathrm{Re}[(j\omega)^{-1}\Psi(\omega)] \geq (\leq) 0$. Now using the series expansion of $\Psi(\omega)$ we obtain

$$\begin{aligned}&\mathrm{Re}[(j\omega)^{-1}\Psi(\omega)] = \\ &\mathrm{Re}[(j\omega)^{-1}D + (j\omega)^{-2}CB + (j\omega)^{-3}CAB + \ldots] = \\ &\mathrm{Re}[(j\omega)^{-1}CA^{-1}B + (j\omega)^{-2}CA^{-1}AB + \ldots] = \\ &\mathrm{Re}[\Phi_R(\omega)]\end{aligned}$$

where the substitution of $(j\omega)^{-1}D$ with $(j\omega)^{-1}CA^{-1}B$ above is valid since

$$\mathrm{Re}[(j\omega)^{-1}D] = \mathrm{Re}[(j\omega)^{-1}CA^{-1}B] = 0$$

□

We now summarize the the results as a theorem connecting the four different phase constraints with the feasibility of four different LMIs.

Theorem 1. Given $A \in \mathbb{R}^{n\times n}$, $B, C^T \in \mathbb{R}^n$, $D \in \mathbb{R}$, with $\det(j\omega I - A) \neq 0$ and (A,C) observable, $\Psi(\omega) = D + C(j\omega I - A)^{-1}B$.

1) $\forall \omega > 0$, $\angle\Psi(\omega) \in \mathscr{P}^{PR}$ iff there exists a $P = P^T \in \mathbb{R}^{n\times n}$ such that

$$\begin{bmatrix} PA^T + AP & B + PC^T \\ B^T + CP & D + D^T \end{bmatrix} \geq 0 \qquad (11)$$

2) $\forall \omega > 0$, $\angle\Psi(\omega) \in \mathscr{P}^{NR}$ iff there exists a $P = P^T \in \mathbb{R}^{n\times n}$ such that

$$\begin{bmatrix} PA^T + AP & B - PC^T \\ B^T - CP & -D - D^T \end{bmatrix} \geq 0 \qquad (12)$$

3) $\forall \omega > 0$, $\angle\Psi(\omega) \in \mathscr{P}^{PI}$ iff there exists a $P = P^T \in \mathbb{R}^{n\times n}$ such that

$$\begin{bmatrix} PA^T + AP & B + P(CA^{-1})^T \\ B^T + CA^{-1}P & 0 \end{bmatrix} \geq 0 \qquad (13)$$

4) $\forall \omega > 0$, $\angle\Psi(\omega) \in \mathscr{P}^{NI}$ iff there exists a $P = P^T \in \mathbb{R}^{n\times n}$ such that

$$\begin{bmatrix} PA^T + AP & B - P(CA^{-1})^T \\ B^T - CA^{-1}P & 0 \end{bmatrix} \geq 0 \qquad (14)$$

3. SUBSPACE ESTIMATE OF A AND C

It is known that the frequency domain subspace techniques formulated directly for continuous-time system are numerically ill-conditioned (McKelvey *et al.*, 1996; Van Overschee and De Moor, 1996). Hence, a reformulation of the problem is required. Here we use the technique described in (McKelvey *et al.*, 1996) which solves the identical identification problem in the discrete time domain. The method is based on the following properties of the bilinear transformation.

- The McMillan degree is unchanged by the transformation.
- Let the continuous-time frequency response be $G(\omega)$ and let $\bar{G}(\bar{\omega})$ denote the discrete-time version. Then for $T > 0$,

$$G(\omega) = \bar{G}(\bar{\omega}), \quad \text{when} \quad \omega = 2\tan(\bar{\omega}/2)/T$$

- If $(\bar{A}, \bar{B}, \bar{C}, \bar{D})$ is the discrete-time state-space realization for $\bar{G}(\bar{\omega})$ then a continuous time realization for $G(\omega)$ is

$$\begin{aligned}&A = \frac{2}{T}(I + \bar{A})^{-1}(\bar{A} - I),\ B = \frac{2}{\sqrt{T}}(I + \bar{A})^{-1}\bar{B} \\ &C = \frac{2}{\sqrt{T}}\bar{C}(I + \bar{A})^{-1}, \qquad D = \bar{D} - \bar{C}(I + \bar{A})^{-1}\bar{B}.\end{aligned} \qquad (15)$$

Using the properties stated above the following technique is used. Assume input/output data samples are given at the continuous-time frequencies ω_k. The necessary steps for the identification of a continuous-time transfer function are:

(1) Select an appropriate value of T, the frequency scaling. As a rule of thumb a value of $T = 5/\max_k \omega_k$ can be used.
(2) Associate the given frequency response at frequency ω_k with the discrete-time frequency

$$\bar{\omega}_k = 2\,\mathrm{atan}(T\omega_k/2) \qquad (16)$$

(3) From the frequency response data and frequencies $\bar{\omega}_k$ estimate a discrete-time state-space model.
(4) Use the transform (15) to obtain the final continuous-time state-space realization.

It should be noted that the conversion to the discrete-time domain, and back is exact and hence do not introduce any systematic errors or approximations.

3.1 *Frequency data*

Frequency data in the form of input output pairs $Y(\bar{\omega}_k)$ and $U(\bar{\omega}_k)$ can in principle be obtained in two different ways.

(i) Through a frequency testing procedure which produces samples of the frequency response function (FRF), so called FRF-data.
(ii) By directly recording time domain samples of the input and output and subsequently using the discrete Fourier transform (DFT) to convert them to the frequency domain.

From the estimated FRF matrices $\hat{G}_r$ an input-output data set is formed as follows: For each FRF frequency sample $r = 0, \ldots, N-1$ and for each input $l = 1, \ldots, m$ let Y_{r*m+l} be column l of matrix G_r and let $U_{r*m+l} = e_l$ where e_l is column l of the $m \times m$ identity matrix. Hence, a set of N FRF-data matrices yields a total of $M = N * m$ input-output data pairs. Each frequency and column in $\hat{G}_k$ thus contributes to one input-output pair $\{Y_k, U_k\}$. The reason for re-shaping the data is to facilitate the use of the same algorithms for both FRF data, as well as directly measured input-output data.

A second alternative to obtain the raw DFT of the recorded input and output data sequences, see (McKelvey, 2000; McKelvey, 2004) for more details.

3.2 *Finding the subspace estimate*

Let us start this section by defining the the extended observability matrix with $q \geq n$ block rows

$$\mathscr{O} = \begin{bmatrix} \bar{C} \\ \bar{C}\bar{A} \\ \vdots \\ \bar{C}\bar{A}^{q-1} \end{bmatrix} \tag{17}$$

and the lower block-triangular Toeplitz matrix

$$\Gamma = \begin{bmatrix} \bar{D} & 0 & \dots & 0 \\ \bar{C}\bar{B} & \bar{D} & \dots & 0 \\ \vdots & \vdots & \ddots & \vdots \\ \bar{C}\bar{A}^{q-2}\bar{B} & \bar{C}\bar{A}^{q-3}\bar{B} & \dots & \bar{D} \end{bmatrix}. \tag{18}$$

An application of the discrete time Fourier transform to the state equations results in the vector relation (McKelvey *et al.*, 1996)

$$\begin{bmatrix} Y(\bar{\omega}) \\ Y(\bar{\omega})e^{j\bar{\omega}} \\ \vdots \\ Y(\bar{\omega})e^{j\bar{\omega}(q-1)} \end{bmatrix} = \mathscr{O}X(\bar{\omega}) + \Gamma \begin{bmatrix} U(\bar{\omega}) \\ U(\bar{\omega})e^{j\bar{\omega}} \\ \vdots \\ U(\bar{\omega})e^{j\bar{\omega}(q-1)} \end{bmatrix} \tag{19}$$

which holds for all $\bar{\omega}$. Using all data samples at the frequencies $\bar{\omega}_k$ for $k = 0, \dots, M-1$, we can merge all the M vector relations into

$$\mathbf{Y} = \mathscr{O}\mathbf{X} + \Gamma\mathbf{U} \tag{20}$$

where column k in (20) corresponds to (19) for $\bar{\omega} = \bar{\omega}_k$. The number of block-rows in $\mathbf{Y}$ is controlled by the auxiliary order q. Since the realization is assumed minimal, the matrix $\mathscr{O}$ defined in (17) has full rank n whenever $q \geq n$, see (Kailath, 1980). Hence, the matrix product $\mathscr{O}\mathbf{X}$ has at most rank n. The output $\mathbf{Y}$ is thus composed of the sum of a low-rank matrix and (in general) a full rank matrix $\Gamma\mathbf{U}$. Since the number of columns in (20) equals the number of data, the matrices become wider as M increases. Let us introduce the notation $\mathbf{Y}^{\text{re}} \triangleq [\text{Re}\,\mathbf{Y},\ \text{Im}\mathbf{Y}]$. Since the state-space realization (A,B,C,D) has real-valued matrices, the complex matrix expression (20) can equivalently be formulated as

$$\mathbf{Y}^{\text{re}} = \mathscr{O}\mathbf{X}^{\text{re}} + \Gamma\mathbf{U}^{\text{re}} \tag{21}$$

which is the basic equation many subspace-based system identification methods use, see e.g. (Viberg, 1995; Liu *et al.*, 1994; McKelvey *et al.*, 1996). In (21) note that only the matrices $\mathbf{Y}^{\text{re}}$ and $\mathbf{U}^{\text{re}}$ are known.

Let us denote by $\Pi^{\perp}$ a matrix which projects onto the null space of $\mathbf{U}^{\text{re}}$ and then multiply this matrix from the right in (21). Since $\mathbf{U}^{\text{re}}\Pi^{\perp} = 0$ we directly obtain $\mathbf{Y}^{\text{re}}\Pi^{\perp} = \mathscr{O}\mathbf{X}^{\text{re}}\Pi^{\perp}$. A numerically efficient and stable way to perform this step is by using QR-factorization (Golub and Van Loan, 1989)

$$\begin{bmatrix} \mathbf{U}^{\text{re}T} & \mathbf{Y}^{\text{re}T} \end{bmatrix} = \begin{bmatrix} Q_1 & Q_2 \end{bmatrix} \begin{bmatrix} R_{11} & R_{12} \\ 0 & R_{22} \end{bmatrix} \tag{22}$$

and noting that $\mathbf{Y}^{\text{re}}\Pi^{\perp} = R_{22}^T Q_2^T$. In the next step a basis of the range space of $\mathscr{O}$ is estimated. The singular value decomposition (SVD) is used for this purpose (Golub and Van Loan, 1989)

$$R_{22}^T = \begin{bmatrix} U_s & U_o \end{bmatrix} \begin{bmatrix} \Sigma_s & 0 \\ 0 & \Sigma_o \end{bmatrix} \begin{bmatrix} V_s^T \\ V_o^T \end{bmatrix}. \tag{23}$$

where $[U_s,\, U_o]$ and $[V_s,\, V_o]$ are two square orthonormal matrices and Σ_s and Σ_o are diagonal matrices with non-negative singular values sorted such that all diagonal entries in Σ_s are larger than the ones in Σ_o and the dimension of Σ_s is selected to be $n \times n$. In our case $\text{rank}\,(R_{22}) = \text{rank}\,(\mathbf{Y}^{\text{re}}\Pi^{\perp}) \leq \text{rank}\,\mathscr{O} = n$, i.e., the rank can at most be n. This implies that $\Sigma_o = 0$. It can be shown that the projection does not decrease the rank any further (McKelvey *et al.*, 1996) so in fact $\text{rank}\,(R_{22}) = n$ and hence all n singular values in Σ_n are positive. Therefore, $R_{22}^T = U_s\Sigma_s V_s^T$ and as an estimate of the extended observability matrix we use $\hat{\mathscr{O}} = U_s$. If we set $T = \mathbf{X}^{\text{re}}\Pi^{\perp}Q_2 V_s \Sigma_s^{-1}$ it is straightforward to verify that $\hat{\mathscr{O}} = U_s = \mathscr{O}T$. Here it is important to point out that only the range space of $\mathscr{O}$ has been calculated. The range space information is, however, enough to recover the transfer function in *some* realization.

The estimates of $\hat{A}$ and $\hat{C}$ are now immediate. Firstly $\hat{C}$ is taken as the first p rows of $\hat{\mathscr{O}}$. Secondly, if we define $\overline{\hat{\mathscr{O}}}$ as the matrix obtained from $\hat{\mathscr{O}}$ by removing the top p rows and defining $\underline{\hat{\mathscr{O}}}$ as the matrix obtained by removing the bottom p rows, it is clear from (17) that $\underline{\hat{\mathscr{O}}}\hat{A} = \overline{\hat{\mathscr{O}}}$, see (Kung, 1978). The matrix $\underline{\hat{\mathscr{O}}}$ has $q-1 \geq n$ block rows and has, as argued previously, full rank. The state-transition matrix is then obtained by

$$\hat{A} = \underline{\hat{\mathscr{O}}}^{+}\overline{\hat{\mathscr{O}}} \tag{24}$$

where the notation $(\cdot)^{+}$ denotes the pseudo-inverse of a matrix (Golub and Van Loan, 1989).

With the discrete time estimates at hand we now proceed by using the bilinear transform (15) to calculate the continuous-time matrices A and C.

4. SOLVING FOR B AND D

We are now in a position that we can obtain estimates of the B and D matrices using a constrained least squares technique, which results in a convex quadratic program.

For each frequency, let us define the error as

$$E_k = Y(\omega_k) - \big(D + C(j\omega_k I - A)^{-1}B\big)\,U(\omega_k). \tag{25}$$

The constrained least-squares problem can now be formulated as

$$\min_{B,D,P_1,\ldots,P_{n_c}} \sum_{k=1}^{M} \|W_k E_k\|^2$$
$$\text{subject to} \quad \angle G_{i_p,j_p}(\omega) \in \mathscr{P}_p, \quad \forall \omega \geq 0 \quad p = 1,\ldots,n_c \tag{26}$$

where W_k is a weighting matrix which can be chosen in order to shape the modeling error. Each of the n_c phase constraints in (26) results in an LMI of the forms (11)-(14), where each of the LMI's has an individual P matrix, P_p, $p = 1,\ldots,n_c$, associated with it. Notice that all the LMI's are affine in the free variables $B, D, P_1, \ldots, P_{n_c}$ and form a convex problem. The least-squares part is a quadratic function of B and D and is identical to a second order cone program. Hence, the constrained problem is convex and is efficiently solved by an interior point method. For the numerical examples in this paper we have used the MATLAB package SeDuMi (Sturm, 1999) together with the LMI parser Yalmip (Löfberg, 2004).

5. IDENTIFICATION OF A CANTILEVER BEAM

5.1 *Experimental testbed*

Experiments were performed on a cantilever beam with two collocated piezoelectric pairs. One pair was located close to the clamped end and the other closer to the free end of the beam. For each collocated pair, one piezoelectric patch was used as an actuator, and was driven by a charge amplifier, while the voltage induced in the other patch was used as the measurement. Another piezoelectric actuator was bonded to the beam, somewhere between the two actuating patches. This transducer was driven by a voltage source to apply a disturbance to the beam. The transducer collocated with this actuator was short circuited so that it would not add any loading on the structure. A Schematic of the experimental testbed is demonstrated in Figure 1, a picture of the actual beam is shown in Figure 2.

The purpose of the experiment was to generate frequency domain data to identify a three-input-three-output model as illustrated in Figure 3. The first input corresponds to the disturbance voltage (w) applied to the middle patch. The second and third inputs are the charges (q_1 and q_2) applied to the first and second actuators respectively. The first output corresponds to the displacement measured at the tip of the cantilever (Y_{tip}). The second and third outputs are the voltages (V_{p_1} and V_{p_2}) measured at the first and second piezoelectric transducers, respectively.

To model the plant we measured all nine frequency responses for each input-output combination. These frequency responses were obtained by applying a sinusoidal chirp signal of varying frequency (from 5 to 250 Hz) to the piezoelectric actuators and measuring the corresponding output signals of interest (namely the output voltages V_p from the collocated sensors and the displacement at the tip of the beam Y_{tip}). The input/output data was processed in real time by the

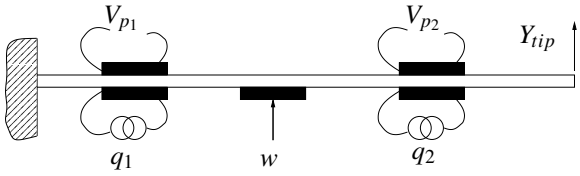

Fig. 1. Beam Arrangement

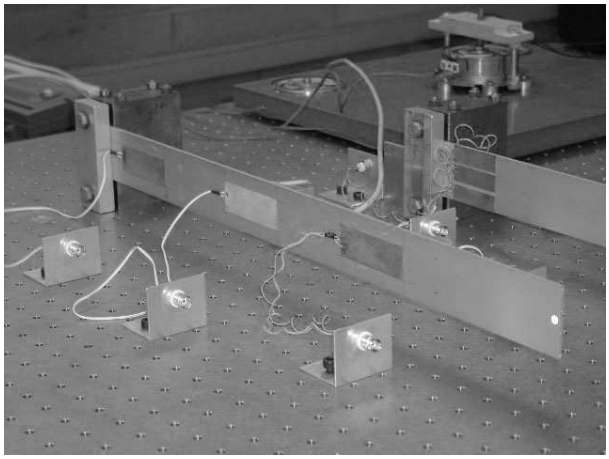

Fig. 2. Picture of the Cantilever Beam

Polytec laser scanning vibrometer (PSV-300) software to obtain the desired frequency responses.

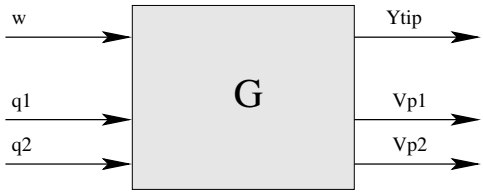

Fig. 3. Augmented MIMO Plant

5.2 *Estimation results*

Data in the frequency range from 5 to 164 Hz is used for the identification. The number of frequency response samples are 2542 where each sample consists of a three by three FRF matrix. The samples are equidistantly spaced in frequency. The subspace approach outlined above is used to calculate A and C matrices of model order 7 from the frequency data. The auxiliary model order q was selected to be 100.

As the second and third sensor-actuator pairs are collocated, the phase curve is, for physical reasons, constrained to stay within a 180 degree range. Due to the amplification equipment used the complex transfer function of the second sensor-actuator pair should be constrained to the positive imaginary half plane ($\angle G_{2,2}(\omega) \in \mathscr{P}^{PI}$) while the third sensor-actuator pair should be constrained to the negative imaginary half plane ($\angle G_{3,3}(\omega) \in \mathscr{P}^{NI}$).

First a straightforward least-squares estimate is made for the B and D matrices. However this unconstrained estimate violates the phase constraints of the physical system. A second B and D pair is then calculated by

solving the convex optimization problem (26) using two LMIs to impose the constraints on the second and third collocated sensor-actuator pairs.

The maximum singular values of the unconstrained and constrained estimates are plotted in Figure 4 together with the singular values of the error between the data and the models. The constrained estimate has, as expected, marginally larger estimation error as compared to the unconstrained estimate. In Figure 5 a zoomed plot of the phase curve of the second sensor-actuator pair is shown. Clearly the unconstrained estimate violates the phase bounds.

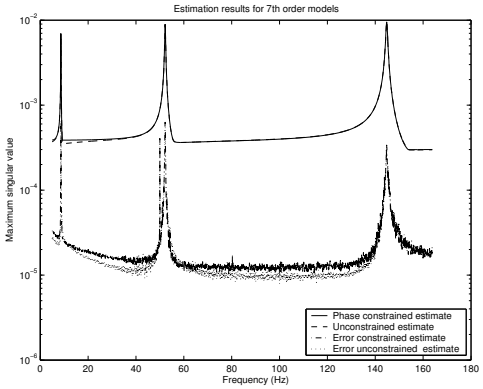

Fig. 4. Singular values of the two estimated transfer functions of order 7 and the singular values of the error between the FRF data and the estimated models. Solid and dash dotted lines: constrained estimate. Dashed and dotted lines: unconstrained estimate.

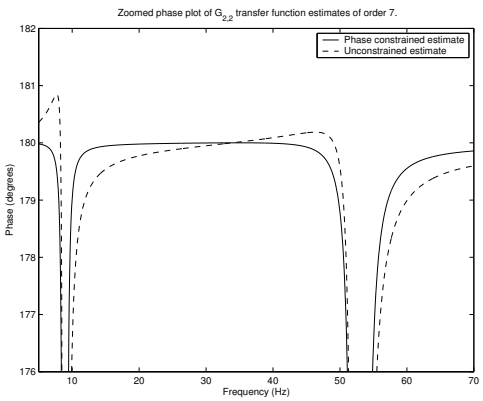

Fig. 5. Zoomed phase plot for the transfer function between the second input and second output which are collocated. Graphs for both the unconstrained and constrained 7th order estimate

6. CONCLUSIONS

An estimation technique has been presented which identifies continuous-time MIMO state-space models from frequency response function data. Furthermore, the technique includes a possibility to individually constrain the complex transfer function elements to have a phase curve which is bounded to either 180 degree or 90 degree segments. The method is a combination of a subspace technique which is used to identify the poles of the system while the zeros are estimated with a constrained least-squares technique which uses a combination of linear matrix inequalities and second order cone programming to find the optimal constrained estimate. The methodology has successfully been applied to data from a cantilever beam with three sensors and three actuators in which two pairs are collocated.

7. REFERENCES

Goethals, I., T. Van Gestel, J. Suykens, P. Van Dooren and B De Moor (2003). Identification of positive real models in subspace identification by using regularization. *IEEE Transactions on Automatic Control* **48**(10), 1843–1847.

Golub, G. H. and C. F. Van Loan (1989). *Matrix Computations*. second ed.. The Johns Hopkins University Press. Baltimore, Maryland.

Jesse, B., Seth L. Lacy, Richard Scott Erwin and Dennis S. Bernstein (2004). First-order-hold sampling of positive real systems and subspace identification of positive real models. In: *Proc. American Control Conference*. pp. 861–866.

Kailath, T. (1980). *Linear Systems*. Prentice-Hall. Englewood Cliffs, New Jersey.

Kung, S. Y. (1978). A new identification and model reduction algorithm via singular value decomposition. In: *Proc. 12th Asilomar Conference on Circuits, Systems and Computers, Pacific Grove, CA*. pp. 705–714.

Liu, K., R. N. Jacques and D. W. Miller (1994). Frequency domain structural system identification by observability range space extraction. In: *Proc. American Control Conference, Baltimore, Maryland*. Vol. 1. pp. 107–111.

Löfberg, J. (2004). YALMIP : A toolbox for modeling and optimization in MATLAB. In: *CCA/ISIC/CACSD*.

Mari, J., P. Stoica and T. McKelvey (2000). Vector ARMA estimation: A realiable subspace approach. *IEEE Trans. on Signal Processing* **48**(7), 2092–2104.

McKelvey, T. (2000). Frequency domain identification. In: *Preprints of the 12th IFAC Symposium on System Identification* (R. Smith and D. Seborg, Eds.). Santa Barbara, CA, USA. Plenary paper.

McKelvey, T. (2004). Subspace methods for frequency domain data. In: *Proc. American Control Conference*. Boston, USA. pp. 673–678.

McKelvey, T., H. Akçay and L. Ljung (1996). Subspace-based multivariable system identification from frequency response data. *IEEE Trans. on Automatic Control* **41**(7), 960–979.

Rantzer, A. (1996). On the Kalman-Yakubovich-Popov lemma. *Systems Control Lett.* **28**(1), 7–10.

Stoica, P., T. McKelvey and J. Mari (2000). MA estimation in polynomial time. *IEEE Trans. on Signal Processing* **48**(7), 1999–2012.

Sturm, J. F. (1999). Using SeDuMi 1.02, a MATLAB toolbox for optimization over symmetric cones. *Optimization Methods and Software* **11-12**, 625–653. Special issue on Interior Point Methods.

Van Overschee, P. and B. De Moor (1996). Continuous-time frequency domain subspace system identification. *Signal Processing, EURASIP* **52**(2), 179–194.

Van Overschee, P., B. De Moor, W. Dehandschutter and J. Swevers (1997). A subspace algorithm for the identification of discrete time frequency domain power spectra. *Automatica* **33**(12), 2147–2157.

Viberg, M. (1995). Subspace-based methods for the identification of linear time-invariant systems. *Automatica* **31**(12), 1835–1851.